International Journal of Pharmaceutics 646 (2023) 123471

Contents lists available at ScienceDirect

International Journal of Pharmaceutics

journal homepage: www.elsevier.com/locate/ijpharm

Flexosomes as a promising nanoplatform for enhancing tolnaftate ocular delivery: Formulation, in vitro characterization, statistical optimization, ex vivo and microbial in vivo studies

Diana Aziz [a], Sally Mohamed [b], Saadia Tayel [a], Amal Makhlouf [a,c,*]

[a] Department of Pharmaceutics and Industrial Pharmacy, Faculty of Pharmacy, Cairo University, Cairo, Egypt
[b] Department of Microbiology and Immunology, Faculty of Pharmacy, Cairo University, Cairo, Egypt
[c] Department of Pharmaceutics and Industrial Pharmacy, Faculty of pharmacy, October University for Modern Sciences and Arts (MSA), Cairo, Egypt

ARTICLE INFO

Keywords:
Flexosomes
Tolnaftate
Stearylamine
Flux
Draize
Susceptibility

ABSTRACT

The eye is a complex organ with a unique physiology and anatomy. Using novel nanosystems is expected to enhance ocular drug permeation and retention. Hence, this work aimed to study the potential of flexosomes as an ocular delivery system to enhance the corneal permeation and antifungal activity of Tolnaftate (TOL). Different flexosomes formulae were formulated using ethanol injection method, employing a $3^1.2^2$ full factorial design. The studied formulation variables were: X_1: amount of stearyl amine, X_2: hydration volume and X_3: type of edge activator. Encapsulation efficiency, particle size and zeta potential were selected as dependent variables. FX5 was selected as the optimal TOL flexosomes and showed encapsulation efficiency of 66.08 ± 11.38%, particle size of 154.99 ± 29.11 nm and zeta potential of 42.95 ± 0.64 mV. FX5 was subjected to further ex vivo and in vivo studies which showed that TOL flux was significantly increased through FX5 compared to TOL suspension. Draize test and histopatholoigal tests assured that FX5 is safe to be used for eye.. The in vivo fungal susceptibility testing using Aspergillus niger demonstrated the superior and more durable antifungal activity of FX5 than TOL suspension. Hence, FX5 can be considered as promising nanocarrier for safe and efficient ocular TOL delivery.

1. Introduction

Around 90% of ocular dosage forms are in form of conventional eye drops due to their rapid action, ease of installation, noninvasiveness which consequently increase patient compliance (Basha et al., 2013; Fetih, 2016). However, only small amount of the applied dose can reach to cornea and intraocular tissues due to natural blinking reflex, nasolacrimal drainage and rapid tear turnover which cause premature corneal drug elimination (Eldeeb et al., 2019). Therefore, the currently available ocular therapies are of limited efficacy and low bioavailability and require frequent dosing to maintain the therapeutic drug level in eye which reduces the patient compliance.

The use of colloidal nanocarriers (e.g., niosomes, liposomes and mixed micelles) has been intensively investigated in the last two decades to enhance the drug corneal permeation, prolong drug residence time in the eye, prevent the enzymatic metabolism of the drug at the tear/corneal surface and consequently enhance drug bioavailability (Li et al., 2018). Recently, modulating the composition of the previously mentioned conventional nanocarriers has been extensively studied for developing especially designed elastic nanocarriers like spanlastics and transferosomes for enhancing the drug penetration through biomembranes (skin, cornea, etc.) (Basha et al., 2013; ElMeshad & Mohsen, 2016). These elastic vesicles are expected to be more advantageous over the classical counterparts due to the high elasticity of their vesicular membrane which is estimated to facilitate their squeezing through pores much smaller than their sizes with resultant enhanced drugs bioavailability (Naguib et al., 2017).

Transferosomes, fashioned by adding edge activator to liposomal phospholipid, are hypothesized to be with unique ultra-flexible properties to cross biological membranes with high deformability. Edge activators, being surfactants, can destabilize the vesicular lipid bilayer, increase its fluidity and consequently improve the drug delivery through biological membranes (Di Marzio et al., 2012). Furthermore, the metastable features of edge activators can provide the vesicular membrane with self-optimizing deformability to squeeze through membrane pores smaller than their own diameters when applied under non-occlusive

* Corresponding author at: Department of Pharmaceutics and Industrial Pharmacy, Faculty of Pharmacy, Cairo University, Kasr El-Aini, 11562 Cairo, Egypt.
E-mail address: Amal.Makhlouf@pharma.cu.edu.eg (A. Makhlouf).

https://doi.org/10.1016/j.ijpharm.2023.123471
Received 25 July 2023; Received in revised form 24 September 2023; Accepted 30 September 2023
Available online 2 October 2023

conditions (Gupta et al., 2012). Therefore, transferosomes, compared to classical liposomes, can respond to the external stress by spontaneous shape transformation with resultant avoidance of vesicular rupture (Gonzalez-Rodriguez et al., 2016). With respect to liposomal charge, it was stated that the probability of vesicular aggregation and fusion is lower for charged liposomes than uncharged ones. Furthermore, positively charged liposomes provide higher drug delivery with longer duration of action compared to negatively charged liposomes (Agarwal et al., 2016). This is due to the intimate interaction of positively charged liposomes with negatively charged cornea which consequently can prolong drug residence time (Law et al., 2000). It is also stated that corneal epithelium is coated with negatively charged mucin. So, cationic liposomes can be strongly adsorbed to the negative charges of the mucus with resultant slowing down drug drainage by lacrimal fluid (Agarwal et al., 2016). Consequently, formulating novel flexosomes (positively charged transferosomes) is hypothesized to have promising ultra-deformable properties and enhanced corneal adhesion and retention for efficient drug delivery due to the presence of edge activator and positively charged lipids in their constructs. Therefore, studying flexosomes as novel vesicular nanosystem is necessary for optimizing drug delivery to various eye tissues.

Tolnaftate (TOL) is an antifungal drug selectively fights filamentous fungi e.g., Aspergillus spp. It inhibits squalene epoxidase which is an important enzyme for ergosterol biosynthesis (a key component for fungal membrane). As a result, squalene will accumulate in plasma membrane and ergosterol will be lessened which negatively affect membrane permeability and fungal growth (Abousamra & Mohsen, 2016). Mycotic keratitis caused by Aspergillus spp. are common and if not detected early, it can cause choroidal and retinal damage with consequent reduction in the visual capacity (Spadea & Giannico, 2019). Furthermore, Aspergillus spp. developed resistance to dry and hot conditions which significantly increased fungal keratitis caused by these species over the last few years (Sherwal & Verma, 2008). Hence, TOL is expected to be a talented molecule for treating fungal keratitis due to its selective fungicidal properties, lipophilicity (log P 5.5) and its intermediate molecular weight (307.4) which enhance its permeation across lipid rich corneal cell membrane (Kaur et al., 2008). However, TOL low aqueous solubility (0.00054 mg/mL) and penetration together with unique ocular barrier limit its ocular efficacy (Akhtar et al., 2016). Hence; to efficiently eradicate fungal infection, long term use and frequent dosing are required which are the major limitation in treating fungal infection as they not only reduce patient compliance but also increases the probability of developing drug resistance and infection recurrence (Zhu et al., 2023).

Therefore, this work is aiming at formulating TOL in an efficient delivery system to increase its aqueous solubility and enhance its ocular retention and permeation. Our research team formulated TOL in two different novel nanocarriers, cosolvent-modified spanlastics and polymeric pseudorotaxans, which showed superior antifungal properties, ocular permeation and retention capacity over TOL suspension (Aziz et al., 2022a; Aziz et al., 2022b). Up to date, there is no satisfactory data about the use of flexosomes for ocular drug delivery. Therefore, the work in this research aimed at optimizing the ocular administration of TOL for fungal infection treatment via loading into novel flexosomes. The ultra-deformable character of flexosomes achieved by the incorporation of edge activator in addition to the presence of phospholipids and surfactants maximizes the corneal penetration of the drug. In addition, the sustained release pattern of the TOL from flexosomes would increase the contact time of the drug with the cornea and minimize the frequency of administration which increases patient compliance. For achieving this purpose, TOL flexosomes were formulated according to a full $3^1.2^2$ factorial design, the effect of formulation variables on the physicochemical properties of flexosomes was studied and the optimal formula was selected for further investigations.

2. Experimental section

2.1. Materials

Tolnaftate (TOL) was granted by Hikma pharmaceuticals (Cairo, Egypt). Stearyl amine was purchased from Fluka Chemical Co., Germany. Cremophor RH 40 was obtained from BASF Co. (Florham Park, NJ, USA). L-a-phosphatidylcholine (PC) from egg yolk and Tween 80 (polyoxyethylene sorbitan monooleate) were obtained from Sigma Chemical Co., USA. Methanol and absolute alcohol were purchased from El-Nasr Pharmaceutical Chemicals Co. (Abu-Zaabal, Cairo, Egypt).

2.2. TOL flexosomes formulation

Two different edge activators with different HLB values were used for preparing TOL flexosomes by ethanol injection method at PC: edge activator weight ratio of 2:1 (total weight 400 mg). Briefly, absolute ethanol (5 mL) was used to dissolve TOL (10 mg) and PC together with different amounts of stearyl amine with the aid of sonication (5 min at 80°C) to obtain a clear solution. Then, using a 30-gauze syringe, the resultant clear solution was added to aqueous solution of Tween 80 or Cremophor RH 40 as edge activators which previously dissolved in ultrapure distilled water (5 or 10 mL) and heated to 80°C at 600 rpm. Stirring was continued for 30 min at 80°C. Turbid solution of flexosomes were formed spontaneously. Then the resultant flexosomes solution was left on magnetic stirrer at room temperature until complete ethanol evaporation (approximately 30 min). For particle size reduction, the obtained dispersion was then subjected to bath sonication at 25°C for 10 min. Finally, the prepared flexosomes formulae were fully characterized after leaving to equilibrate overnight at 4°C for further characterization.

2.3. Experimental design

TOL flexosomes were fashioned based on full $3^1.2^2$ factorial design using Design-Expert® software (Version 7, Stat-Ease, Inc., Minneapolis, MN, USA). We examined 3 variables in this design; X_1: three levels of amount of stearyl amine, X_2: two levels of hydration volume and X_3: two levels of type of edge activator. We selected EE% (Y_1), PS (Y_2) and ZP (Y_3) as dependent variables. For the amount of stearyl amine (X_1), post-hoc analysis was performed using Tukey's HSD test using SPSS software 17.0 (SPSS Inc., Chicago, IL). Table 1 present the studied factors and their levels. Table 2 demonstrate the design matrix of TOL flexosomes (including the composition of the prepared formulae along with their full characterization).

2.4. In vitro evaluation of TOL flexosomes

2.4.1. Encapsulation efficiency (EE%)

EE% of TOL in flexosomes was determined by quantifying the amount of entrapped drug by filtering the formula using Whatman filter paper to remove the unentrapped drug (grade No. 1, 11 μm) (Fahmy

Table 1
Full factorial design ($3^1.2^2$) used for optimization of TOL flexosomes.

Factors (independent variables)	Levels		
X_1: Amount of stearyl amine (mg)	10	20	30
X_2: Hydration volume (mL)	5	10	
X_3: Type of edge activator	Tween 80		Cremophor RH 40
Responses (dependent variables)	**Desirability Constraints**		
Y_1: EE%	Maximize		
Y_2: PS (nm)	Minimize		
Y_3: ZP (mV)	Maximize (as absolute value)		

Abbreviations: EE%, entrapment efficiency percent; PS, particle size; ZP, zeta potential; TOL flexosomes, tolnaftate flexosmes.

Table 2
Experimental runs, independent variables, and measured responses of the $3^1.2^2$ full factorial experimental design of TOL flexosomes.

Formula code*	X_1 Amount of stearyl amine (mg)	X_2 Hydration volume	X_3 Type of edge activator	EE (%)	PS (nm)	PDI	ZP (mV)
FX 1	10	5	Tween 80	46.58 ± 8.81	286.65 ± 13.36	0.349 ± 0.12	+32.15 ± 1.34
FX 2	20	5	Tween 80	47.04 ± 1.12	272.20 ± 4.38	0.324 ± 0.11	+44.00 ± 1.27
FX 3	30	5	Tween 80	68.11 ± 0.81	254.85 ± 0.21	0.290 ± 0.10	+46.10 ± 4.38
FX 4	10	5	Cremophor RH 40	48.45 ± 4.45	320.05 ± 10.39	0.454 ± 0.04	+30.45 ± 4.17
FX 5	20	5	Cremophor RH 40	66.08 ± 11.38	154.99 ± 29.11	0.442 ± 0.14	+42.95 ± 0.64
FX 6	30	5	Cremophor RH 40	45.56 ± 2.56	289.40 ± 2.97	0.397 ± 0.10	+46.20 ± 2.12
FX 7	10	10	Tween 80	53.77 ± 0.25	235.20 ± 0.14	0.476 ± 0.03	+4.16 ± 0.42
FX 8	20	10	Tween 80	48.73 ± 4.81	195.30 ± 3.54	0.438 ± 0.15	+24.05 ± 0.78
FX 9	30	10	Tween 80	60.52 ± 4.81	113.00 ± 5.23	0.408 ± 0.12	+31.50 ± 0.57
FX10	10	10	Cremophor RH 40	40.65 ± 6.58	236.30 ± 16.40	0.327 ± 0.01	+25.20 ± 1.56
FX11	20	10	Cremophor RH 40	44.52 ± 1.15	147.90 ± 2.83	0.299 ± 0.02	+47.25 ± 1.63
FX12	30	10	Cremophor RH 40	36.94 ± 0.96	454.95 ± 49.43	0.282 ± 0.08	+55.85 ± 0.21

Abbreviations: EE%, entrapment efficiency percent; PS, particle size; PDI, polydispersity index; ZP, zeta potential; TOL flexosomes, tolnaftate flexosomes.
[a]Data represented as mean ± SD (n = 3).

et al., 2018). Then 0.3 mL of the filtrate was sonicated in methanol then the entrapped TOL concentration was measured spectrophotometrically (λ_{max} 257 nm). The results were presented as mean of three measurments ± SD. Drug EE% was calculated using the following equation:

$$EE\% = \frac{encapsulatedamountofTOL}{TotalamountofTOL} \times 100$$

2.4.2. Particle size (PS), polydispersity index (PDI) and zeta potential (ZP)

The mean PS, PDI, and ZP of the prepared TOL flexosomes were analyzed by Zetasizer Nano ZS (Malvern Instrument Ltd., Worcestershire, UK). For obtaining, the suitable scattering intensity, the prepared dispersions were properly diluted with de-ionized water before each measurement. ZP measurement was performed using the same instrument to observe the particles' electrophoretic mobility in the electric field. Each measurement were repeated 3 times.

2.5. Optimization of TOL flexosomes

By applying desirability function in Design-Expert® software, the optimal TOL flexosomes were selected. The optimization plan was to select the system with the highest EE% and ZP (as absolute value) and the least PS (Table 1). The formula of the highest desirability value (≈1) was selected to be investigated. To check the validity of the predicted responses given by the software, the selected TOL flexosomes formula was prepared and compared with the observed ones (Fares et al., 2018).

2.6. Transmission electron microscopy (TEM)

TEM was adopted to visualize the morphology of the optimal TOL flexosomes. One drop of flexosomal dispersion was put on a carbon coated copper grid and left at room temperature to dry for 10 min before it was investigated by Joel TEM (Joel JEM 1230, Tokyo, Japan) (Khalil et al., 2017).

2.7. Differential scanning calorimetry (DSC)

Thermal analysis for pure drug, PC, stearyl amine, edge activator, TOL flexosomes and a physical mixture of the formulation components was performed by DSC-60, Shimadzu Corp., Kyoto, Japan. The calorimeter was calibrated using 99.9% indium. Samples (≈ 5 mg) were mounted in aluminum pans and heated to 300 °C at a rate of 10 °C/min under nitrogen purging (25 mL/min).

2.8. Ex vivo studies

2.8.1. Corneas preparation

The study protocol was approved by the Research Ethics Committee, Faculty of Pharmacy, Cairo University, Egypt (PI 2982). Corneas extracted from adult male New Zealand albino rabbits (2.5–3.0 kg) were used in this study. For extracting corneas, the rabbits were anesthetized by intramuscular injection of ketamine 35 mg/kg (anesthetic agent) and xylazine 5 mg/kg (as relaxing agent) then the rabbits were decapitated (Eldeeb et al., 2019). The eyes were then enucleated and the corneas were separated from the globes, rinsed with saline and examined for being intact before mounting. After 30 min of corneal extraction, the corneas can be used in the permeation experiment (Kakkar & Kaur, 2011).

2.8.2. Corneal permeation study

The separated corneas were packed between the receptor and donor compartments of a modified Franz diffusion cell (0.64 cm^2). The corneal surface served as donor compartment and was loaded with accurate volume of each of optimal TOL flexosomes formula and TOL aqueous suspension (each containing 300 μg TOL) under non-occlusive condition. The receptor compartment consisted of 100 mL of methanol: water (3:2) and was kept under continuous stirring (100 rpm at 37 °C) (Sayed et al., 2018). At predetermined time intervals, samples (3 mL) were taken from the receptor compartment at different time intervals (0.5, 1, 2, 4, 6 and 8 h) then fresh medium was immediately added in equal volume. The results of the study were presented as mean of three measurements ± SD. A validated HPLC method was used to quantify the amount of TOL in the withdrawn samples. The amount of permeated TOL (μg/cm^2) was plotted against time (h) and the following equations were used to obtain the flux (J_{max}) and the enhancement ratio (ER) (El Zaafarany et al., 2010).

$$J_{max} = \frac{Amount\ of\ drug\ permeated}{Time \times Area\ of\ membrane}$$

$$ER = \frac{J_{max}\ of\ the\ optimal\ nano\ formulation}{J_{max}\ of\ the\ drug\ suspension}$$

The results were statistically analyzed by one-way ANOVA followed by Post-hoc analysis using Tukey's HSD test at $p < 0.05$.

2.8.3. HPLC determination

A modified isocratic HPLC analytical method was utilized for TOL determination (Kezutyte et al., 2010). The HPLC system (Shimadzu, Kyoto, Japan) consisted of reversed C18 column (X Terra ™ 4.6 mm × 250 mm) packed with 5 μm adsorbent as stationary phase (Waters Corporation, Milford, Massachusetts, USA), L-7110 pump and L-7420 UV detector. The column temperature was kept at 25.0 ± 2.0 °C. The mobile phase was set to be methanol 80% (v/v) with 1.2 mL/min flow rate. TOL was eluted at 6 min and was detected at 258 nm. A calibration curve was constructed in the range of 2–14 μg/mL. The assay was proved valid regarding linearity, accuracy and precision.

2.9. In vitro antifungal activity

2.9.1. Fungal strain and inoculum preparation

Aspergillus niger standard strain (ATCC32656) was selected for this study. Sabouraud dextrose agar (SDA) (Oxoid, Hampshire, UK) was used for cultivation of the fungal strain and incubated for 48–96 h at 28 °C ± 2. In sterile normal saline solution, the germinating spores were harvested and the inoculum size was adjusted to 10^5–10^6 CFU/mL applying a constructed correlation between the viable count and the optical density.

2.9.2. Tested samples

Samples tested for the in vitro antifungal activity were; TOL flexosomes (treatment A), TOL 2 mg/mL suspension (treatment B) and TOL-free flexosomes (placebo).

2.9.3. Minimum inhibitory concentration (MIC)

A method described by Alastruey-Izquierdo et al. (Alastruey-Izquierdo et al., 2015) was applied for the determination of MIC in accordance with the Clinical and Laboratory Standards Institute guidelines (Humphries et al., 2018b). In double strength sabouraud dextrose broth, two-fold serial dilutions of each of treatment A and B were prepared (1000-0.49 μg/mL). Afterwards, spore suspension (10 μL of inoculum size of 10^5–10^6 CFU/mL) was added to each well. Double strength sabouraud dextrose broth only (negative control) and double strength sabouraud dextrose broth and placebo solution with the inoculum (positive control) were also included. The samples were incubated for 48 h at 28 °C ± 2. The MIC was determined as the lowest concentration showing no fungal growth. The experiment was carried out three independant times.

2.9.4. Minimum fungicidal concentration (MFC)

Broth microdilution method was applied for the determination of MFC for treatments A and B in accordance with the Clinical and Laboratory Standards Institute guidelines (Humphries et al., 2018a). In brief, treatment A or B at different concentrations mixed with fungal spore suspension (10 μL) were incubated at 28 ± 2 °C for 24 h in 96-well plates. Samples of the mixture (10 μL) were then spotted on SDA plates, which were incubated for 48 h at 28 ± 2 °C then the fungal colony count was determined as CFU/mL. The lowest concentration showing no fungal growth was taken as the MFC. The experiment was carried out three independant times.

2.9.5. Kill kinetics assay

A modified reported method was used for the determination of kill kinetics of treatments A and B against *Aspergillus niger* (ATCC32656) (Ismail et al., 2020). Shortly, 100 μL of double strength sabouraud dextrose broth, treatment A or treatment B at their MFC concentration and 10 μL of the spore suspension (inoculum size of 10^5–10^6 CFU/mL) were mixed in a 96- well plate,. Sample of this mixture (10 μL) were then blended with 90 μL of saline solution, serially diluted (10 folds) and viable colony count was done on SDA medium (0 time sample). Then the plate was incubated for 24 h at 28 ± 2 °C. Samples were taken after 4, 6, 10, 16, and 24 h, diluted and subjected to viable colony count on SDA medium. The experiment was carried out three times.

2.10. In vivo studies

2.10.1. Animals

The animal study protocol was approved by the Research Ethics Committee at Faculty of Pharmacy, Cairo University, Egypt (PI 2982). Twelve male albino rabbits (2 – 3 kg) were adopted in the study. Appropriate housing conditions were adjusted with respect to temperature (25 °C ± 2), humidity and light/dark cycling. Animals were kept on a standard dry food and water ad libitum. A slit lamb was used to examine rabbits and any animal that showed signs of disease or ocular inflammation was excluded.

2.10.2. Draize test

To evaluate the irritation potential of TOL flexosomes, a scoring system was applied.(Eldeeb et al., 2019) New Zealand albino male rabbits (three animals) were included in this test. Sample of 100 μL of the optimal TOL flexosomes was instilled in the conjunctival sac of the right eye of the rabbit and the left eye served as control by installing normal saline. After 1,2,5,8,24,h of installation, the right eye was observed visually and given a score according to Draize test (ElMeshad & Mohsen, 2016; Eldeeb et al., 2019). The test score system extended from zero denoting the absence of any signs of irritation to + 3 denoting the most severe irritation and redness observed.

2.10.3. Histopathological study

New Zealand male albino rabbits (three animals) were employed to assess the safety of TOL flexosomes optimized formula. TOL flexosomes was dropped into the right eye and the left eye was kept as control. The installation was repeated every hour for a period of 6 h (Yousry et al., 2020). The eyeballs were extracted after animals' euthanasia under anesthesia. The eyeballs were thoroughly washed and fixed in 10% formalin in saline. afterwards, they were dehydrated by serial dilutions of alcohol. Tissue blocks in paraffin wax of 4 μm thickness were prepared using a microtome (Leica Microsystems SM2400, Cambridge, England). Tissue sections were put on glass slides, stained with hematoxylin and eosin then examined under light microscope (Bancroft et al., 1996).

2.10.4. Susceptibility test

Susceptibility test was performed on *Aspergillus niger* (ATCC32656) applying a parallel design that involved two groups of male albino New Zealand rabbits each of three animals. The first group received TOL flexosomes (Treatment A) and the second one received TOL suspension (Treatment B) (Albash et al., 2021). Using micropipette, a volume equivalent to 50 μg TOL of treatment A or B was dropped in the lower conjunctival sac of the rabbit's right eye and the left eye served as control. At predetermined times over 24 h, two sterile filter paper discs (6 mm in diameter,Whatman no. 5) were placed under the eyelid of each rabbit eye. The two discs of the right eye were put in an Eppendorf tube containing 10% v/v fungal spore suspension in 500 μL SDB (10^5–10^6 CFU/mL). The two discs of the left eye were added to 500 μL uninoculated SDB in another Eppendorf tube to be used as blank for the optical density measurement. All tubes were incubated for 48 h at 28 °C ± 2 under aerobic conditions. At the end of the incubation time, 200 μL of each tube was added to a 96-well plate to measure the optical density (OD_{600nm}) using a plate reader (Biotek, Synergy 2, USA). The given readings were used to calculate the growth inhibition (%) using the following equation:

$$Growth inhibition\% = \frac{Control\,(left\,eye)\,OD600nm - Test\,(right\,eye)\,OD600nm}{Control\,(left\,eye)\,OD600nm} \times 100$$

3. Results and discussion

3.1. Statistical design analysis

Twelve TOL flexosomes formulations were fashioned according to $3^1.2^2$ full factorial design. It was statistically studied using Design-Expert® software. The levels were selected based on preliminary experiments and possibility of preparing TOL flexosomes applying these levels. Two factor interaction was the selected model. The signal to noise ratio was expressed by the adequate precision to make sure that the model can be used to navigate the design space (Younes et al., 2021). The desired value of this ratio is to be greater than 4 which was recorded for all measured responses (Table 3). The predicted R^2 values came in good agreement with the adjusted values in all responses which confirmed the adequate fitting of the selected model to the data (Table 3).

Table 3
Output data of the $3^1.2^2$ factorial analysis of TOL flexosomes.

Responses	R^2	Adjusted R^2	Predicted R^2	Adequate precision	Significant factors
EE%	0.8103	0.6883	0.4425	8.439	X_2 (=0.0193), X_3 (=0.0085)
PS (nm)	0.8173	0.6998	0.4630	8.244	X_1 (=0.0069)
ZP (mV)	0.9874	0.9794	0.9631	40.414	X_1 (<0.0001), X_2(<0.0001), X_3(<0.0001)

Abbreviations: EE%, entrapment efficiency percent; PS, particle size; ZP, zeta potential.

3.1.1. *Effect of formulation variables on EE% of TOL flexosomes*

The entrapment efficiency of TOL flexosomes ranged from 36.94 ± 0.96 to 68.11 ± 0.81% as shown in Table 2. The influence of amount of stearyl amine (X_1), hydration volume (X_2) and type of edge activator (X_3) on EE% of TOL flexosomes was graphically presented in Fig. 1. ANOVA results (Table 3) revealed that EE% of TOL flexosomes was not affected significantly by stearyl amine amount (X_1) ($P = 0.1773$). On the other hand, hydration volume (X_2) had a statistically significant effect ($P = 0.0193$) on EE%. This might be explained by that we used a fixed amount of TOL in each preparation (10 mg). Thus, by decreasing hydration volume, TOL concentration increased with consequent increase in EE%. This could be attributed to the saturation of hydration medium with TOL which forces the drug to be entrapped into flexosomes (Balakrishnan et al., 2009; Abdelbary & AbouGhaly, 2015). Furthermore, with a constant total lipid mass (400 mg) in all formulations, the increase in final lipid concentration with decreasing hydration volume caused noticeable increase in EE%. This could be related to that increasing total lipid concentration will make the vesicular membrane less permeable which consequently promotes EE% (Hichmah, 2019; Yeo et al., 2019). In other words, it was reported that increasing hydration volume increased the drug leakage and consequently decreased EE% (Ruckmani & Sankar, 2010; Abdelbary & AbouGhaly, 2015). With respect to the type of edge activator (X_3), flexosomes prepared using Tween 80 as edge activator showed higher EE% compared to those prepared using Cremophor RH 40 ($P = 0.0085$). Although both edge activators utilized have similar HLB values (14–16), Cremophor RH 40-based vesicles showed significantly lower EE% due to its more branched structure which resulted in development of steric hindrance that prevented the proper aggregation of surfactant molecule to form tightly closed vesicles (Arunothayanun et al., 2000; Abdelbary & Aburahma, 2015). The chemical structures of both edge activators are presented in Table 1S.

3.1.2. *Effect of formulation variables on PS of TOL flexosomes*

Particle size of TOL flexosomes ranged from 113.00 ± 5.23 to 454.95 ± 49.43 nm as demonstrated in Table 2. The small PS is advantageous in ensuring safe ocular drug delivery with adequate bioavailability. The

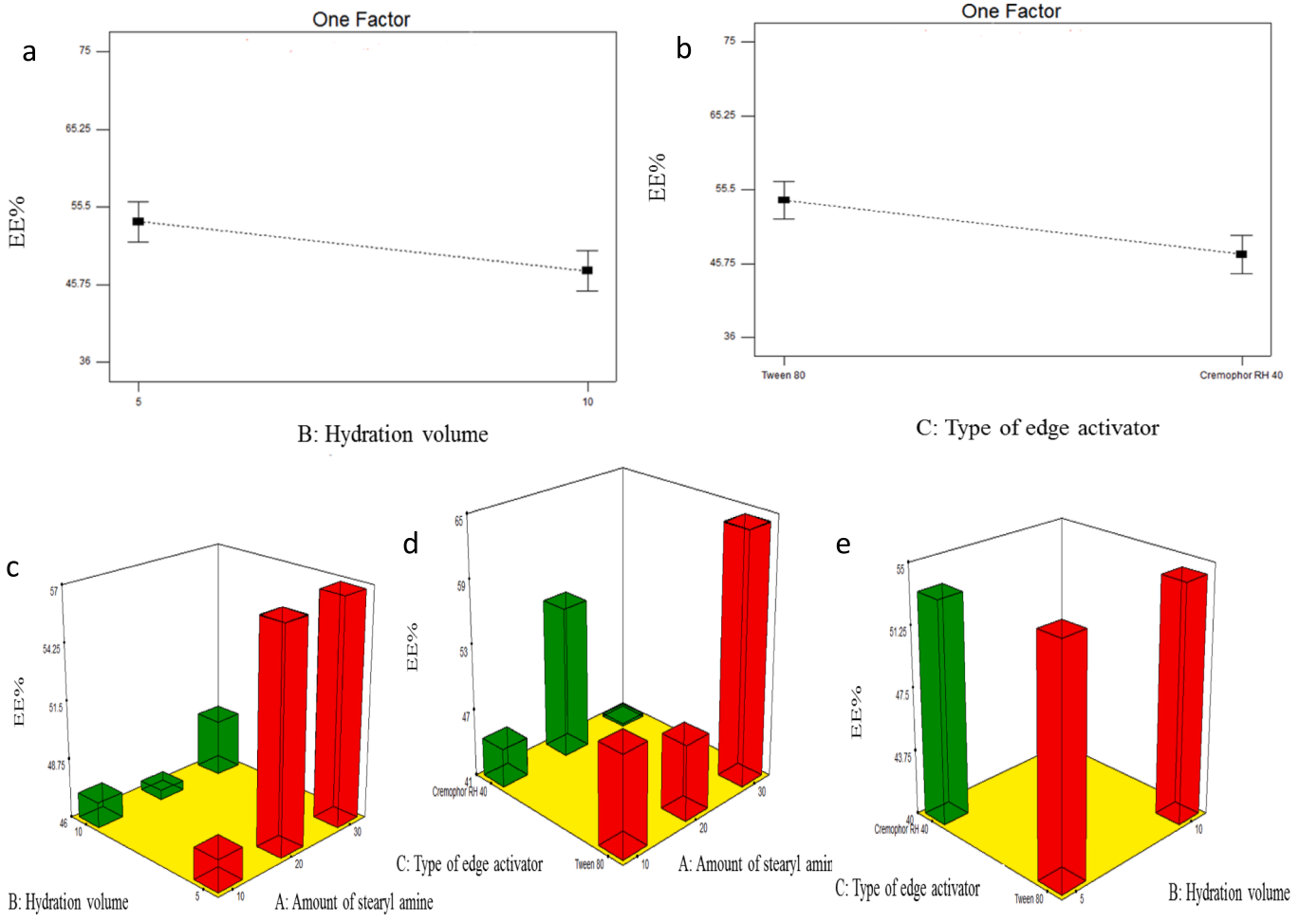

Fig. 1. Line plots of the significant effect of hydration volume (x_2) (a), type of edge activator (X_3) (b), response 3-D plot for the combined effect of amount of stearyl amine (X_1) and hydration volume (X_2) (c), amount of stearyl amine (X_1) and type of edge activator (X_3) (d) and hydration volume (X_2) and type of edge activator (X_3) (e) on EE% of TOL flexosomes.

influence of the amount of stearyl amine (X_1), hydration volume (X_2) and the type of edge activator (X_3) on the particle size of TOL flexosomes is presented in Fig. 2. The results of ANOVA test (Table 3) showed that the amount of stearyl amine only had a statistically significant impact on the particle size of TOL flexosomes ($P = 0.0069$). By initial increase in the amount of stearyl amine from 10 to 20 mg, the mean diameter of flexosomes significantly decreased due to the disproportionate disruption of stearyl amine within the lipid bilayer which may increase the bilayer curvature by the effect on electrostatic repulsion between the ionized head groups and consequently increasing the hydrophilic surface area and producing vesicles with smaller PS (Varshosaz et al., 2003; Balakrishnan et al., 2009; El-Ridy et al., 2011). On the contrary, by further increasing stearyl amine amount, PS significantly increased. This was attributed to that vesicles prepared using higher amount of charge inducer showed more repulsive force between the adjacent bilayers with consequent increased space between them., resulting in the formation of comparatively larger vesicles (Abdelbary, 2011; Naguib & Makhlouf, 2021). Furthermore, it was revealed that by further increase in surface charge, the thickness of the aqueous compartment of the vesicles directly increased due to increasing water uptake within the vesicular bilayer and consequently increasing PS (Aziz et al., 2019). Oppositely, both hydration volume (X_2) and type of edge activator (X_3) didn't have significant effect on particle size of TOL flexosomes ($P = 0.1294$ and 0.0616, respectively).

3.1.3. *Effect of formulation variables on ZP of TOL flexosomes*

Zeta potential is one of the main factors of the physical stability of nanosystems (Nour et al., 2016). There is a direct relation between the electric charge acquired on nanoparticles surface and the repellant forces between particles which has important role to prevent particles aggregation and give more stable dispersion (Honary & Zahir, 2013). Table 2 demonstrates that ZP of TOL flexosomes ranged from 4.16 ± 0.42 to 55.85 ± 0.21 mV. All formulations had positive charge due to the presence of stearyl amine, positive charge inducer, in the constructs of all flexosomal formulations. The influence of amount of stearyl amine (X_1), hydration volume (X_2) and type of edge activator (X_3) on ZP of TOL flexosomes is graphically illustrated in Fig. 3. Based on the investigated design, ZP of TOL flexosomes was significantly affected by all of formulation variables ($P < 0.0001$) (Table 3). By increasing stearyl amine amount (X_1), ZP values significantly increased. This was related to that stearyl amine introduced positive charge through protonation of the basic amine group. Hence, by increasing stearyl amine amount, more amine groups would be protonated and subsequently adsorbed on the vesicular surface leading to higher positive ZP values (Junyaprasert et al., 2008). With respect to hydration volume (X_2), ANOVA results revealed that increasing water volume significantly decreased ZP. As previously mentioned, stearyl amine imparts vesicles with positive charge due to the free amine groups. Therefore, by increasing water to amine ratio, ZP values decreased (Varshosaz et al., 2014). Results also showed that flexosomes prepared using Cremophor RH 40 were with

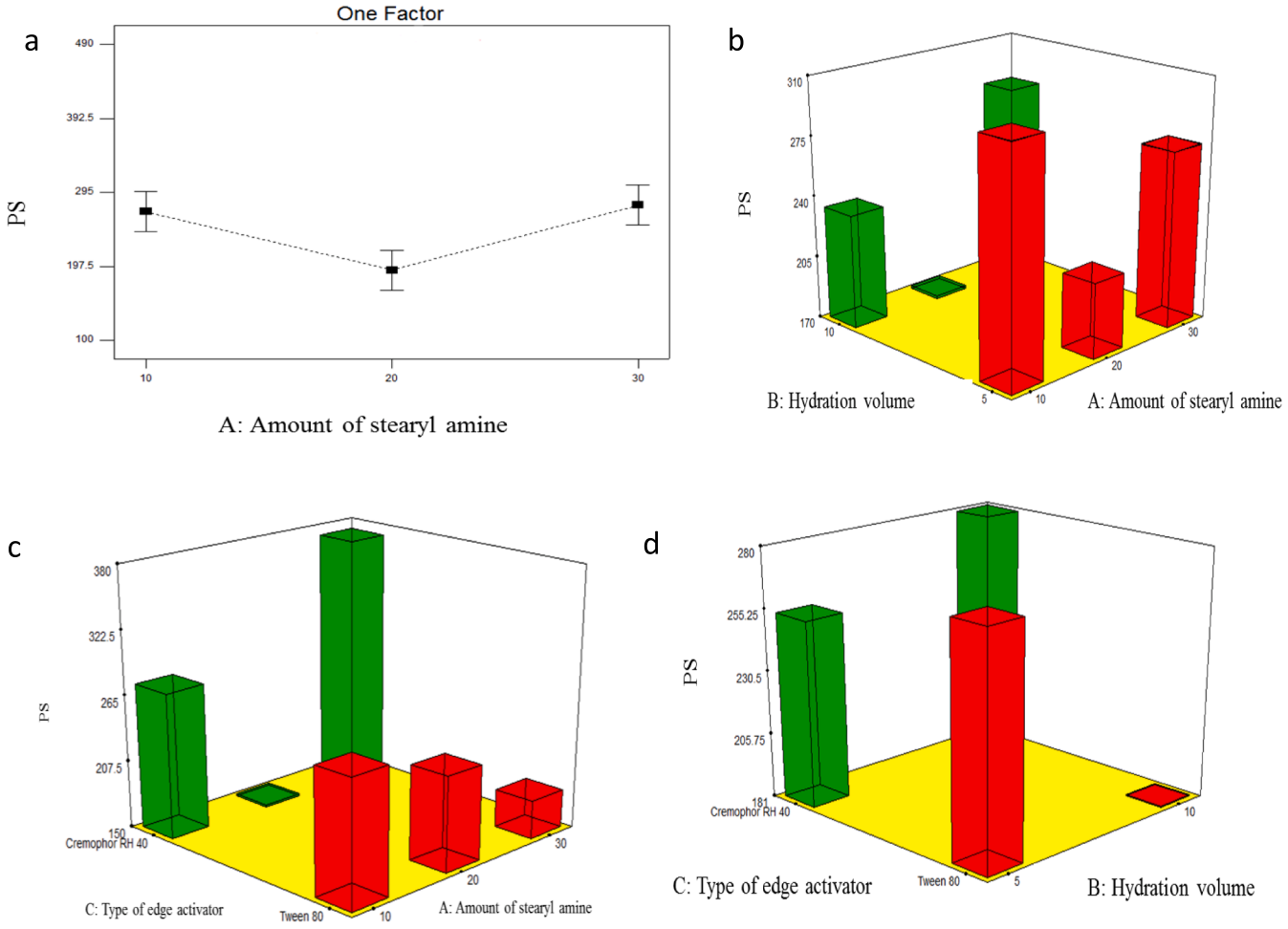

Fig. 2. Line plots of the significant effect of amount of stearyl amine (x_1) (a), response 3-D plot for the combined effect of amount of stearyl amine (X_1) and hydration volume (X_2) (b), amount of stearyl amine (X_1) and type of edge activator (X_3) (c) and hydration volume (X_2) and type of edge activator (X_3) (d) on PS of TOL flexosomes.

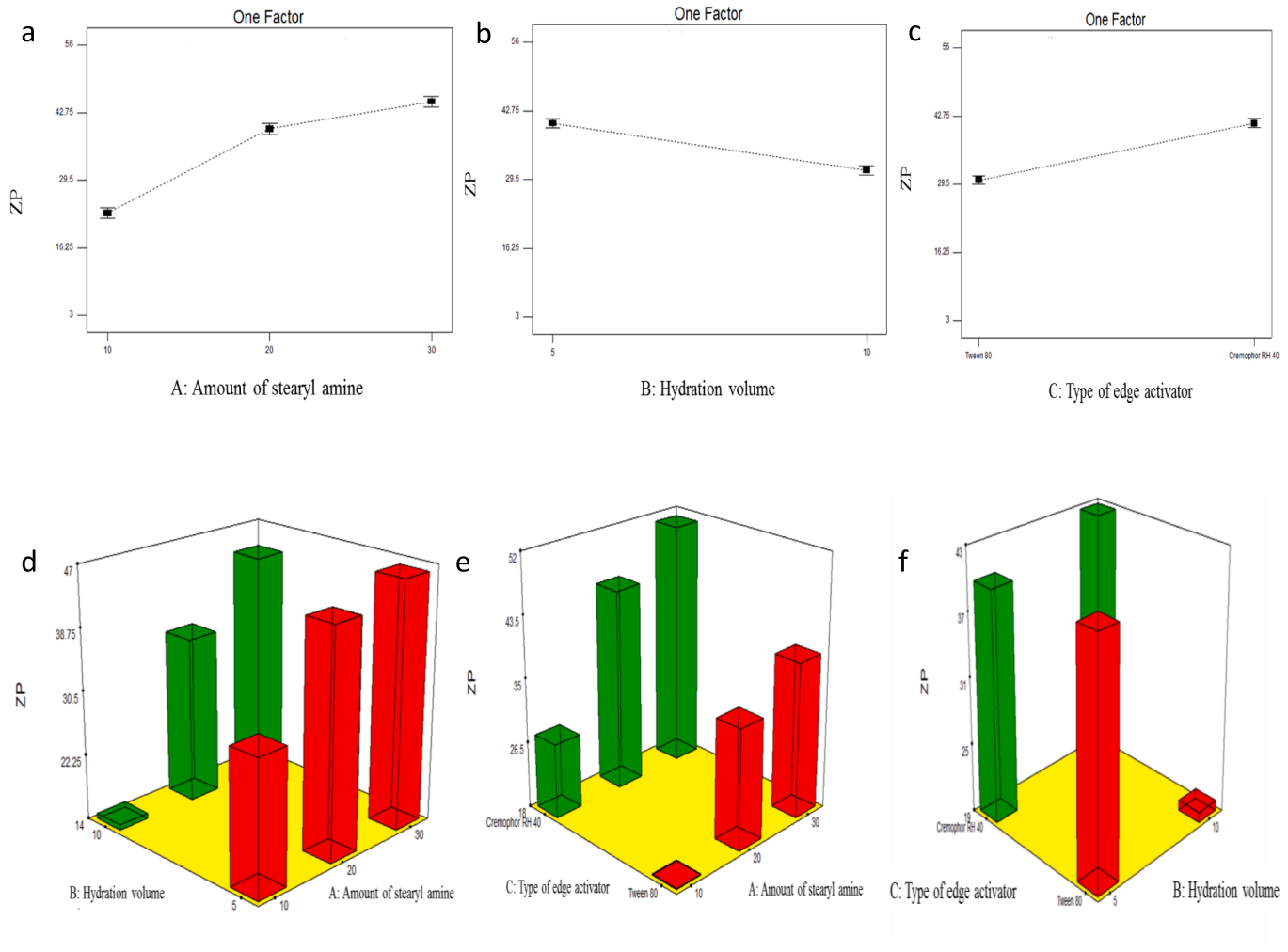

Fig. 3. Line plots of the significant effect of amount of stearyl amine (x_1) (a), hydration volume (X_2) (b), type of edge activator (X_3) (c), response 3-D plot for the combined effect of amount of stearyl amine (X_1) and hydration volume (X_2) (d), amount of stearyl amine (X_1) and type of edge activator (X_3) (e) and hydration volume (X_2) and type of edge activator (X_3) (f) on ZPof TOL flexosomes.

higher ZP values than Tween 80-based vesicles. As previously mentioned under EE% section, vesicles prepared using Tween 80 imparted significantly increased entrapment efficiency in comparison with Cremophor RH40. Therefore, more TOL would be entrapped in Tween 80 based vesicles which ionized and acquired negative charge due to ionization of its thiocarbamate group and consequently caused neutralization of the positively charged amine group of stearyl amine with reduction of net ZP values.

3.1.4. Selection of the optimal TOL flexosomes formulation

The optimization process aims at defining the optimum variables levels from which a promising formulation may be produced (Al-Mahallawi et al., 2014). Hence, desirability function was applied using Design-Expert® software for the selection of the optimum TOL flexosomes formula out of the twelve prepared formulations. According to the desirability constraints (minimum PS and maximum EE% and ZP) were settled in formulation FX5 with desirability value of 0.817. FX5 that was formulated using 20 mg stearylamine, 5 mL hydration medium and Cremophor RH 40 as edge activator. It showed EE% of 66.08 ± 11.38%, PS of 154.99 ± 29.11 nm and ZP of 42.95 ± 0.64 mV. To test the rationality of the optimization, the predicted responses of FX5 were compared to the observed ones (Table 4). The anticipated results obtained using Design-Expert® were in good agreement with the observed results. So, FX5 was subjected to further investigations.

3.2. Transmission electron microscopy

TEM imaging is beneficial to visualize the morphological features of the TOL flexosomes (Abd-Elsalam et al., 2018). As shown in Fig. 4, TEM images of FX5 displayed homogenous spherical small-sized vesicular structure with a smooth non-aggregating surface. Furthermore, there was a good harmony between the flexosomes diameter observed by TEM and that measured by the zetasizer which ranged from100 to 200 nm.

Table 4
Predicted and observed values for the optimal flexosomes (FX5).

Factor		Optimal level
X_1: Amount of stearyl amine (mg)		20
X_2: Hydration volume (mL)		5
X_3: Type of edge activator		Cremophor RH 40
Response	**Expected**	**Observed**
Y_1: EE%	63.47	66.08
Y_2: PS (nm)	143.72	154.99
Y_3: ZP (mV)	43.10	42.95

Abbreviations: EE%, entrapment efficiency percent; PS, particle size; ZP, zeta potential.

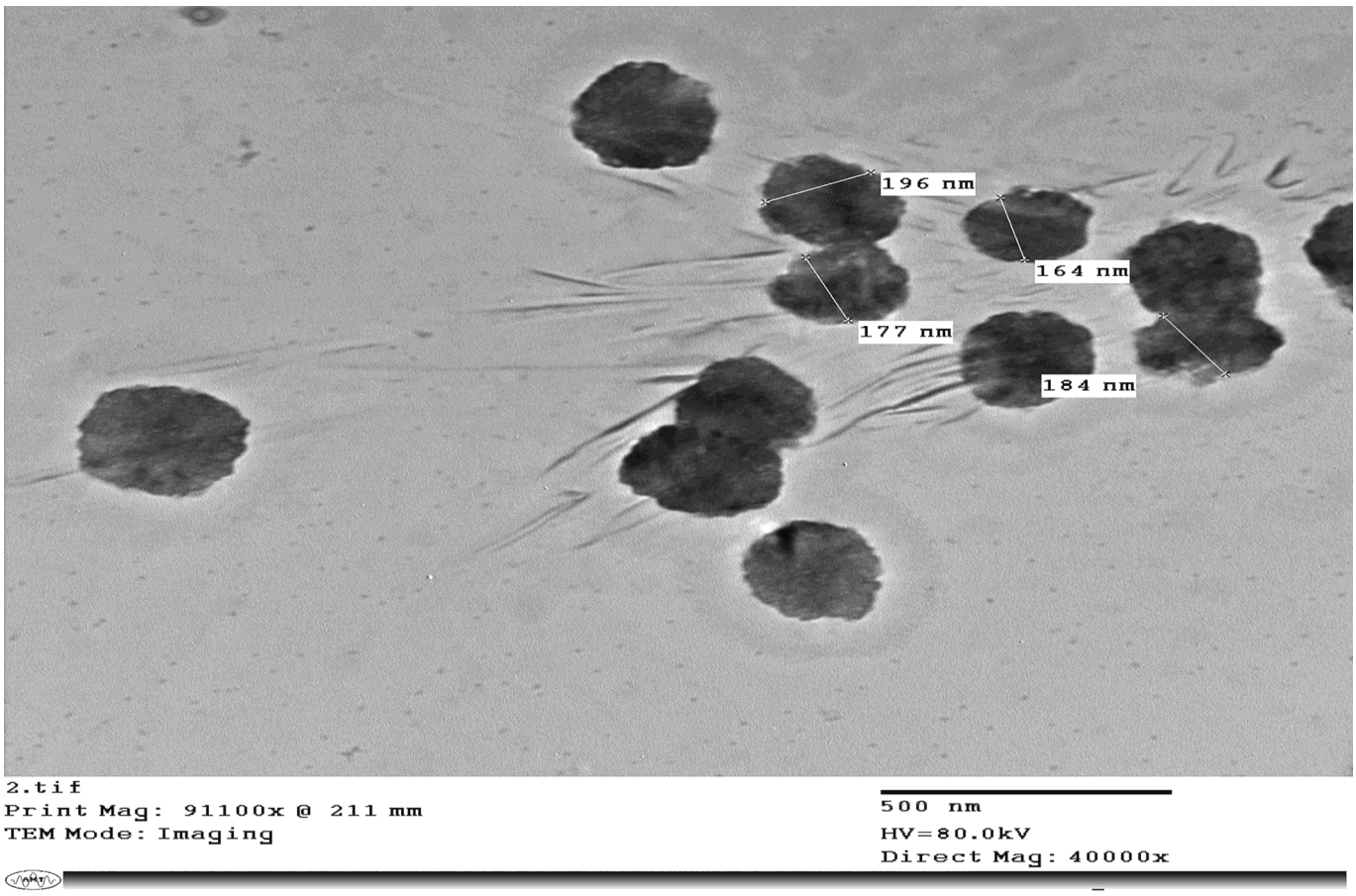

Fig. 4. Transmission electron micrograph of FX5.

3.3. Differential scanning calorimetry

A sharp endothermic peak at 112.31 °C was observed in the DSC thermogram of pure TOL corresponding to its melting point (Kumari et al., 2017). This sharp peak also indicated the crystallinity of TOL. DSC scan of Cremophor RH 40 and stearyl amine depicted endothermic peaks at 141.81 °C and 88.79 °C corresponding to their melting point, respectively. The thermogram of phospholipid showed endothermic peaks at 44.16 °C and 239.83 °C. The peak observed at 44.16 °C indicated the transition temperature (T_m) at which the gel phase of lipid converted to the liquid crystalline state. The peak observed at 239.83 °C might be attributed to the isotropic liquid phase of the phospholipid (Yusuf et al., 2014). The endothermic peak of TOL was preserved in the physical mixture. On the other hand, disappearance of TOL melting endotherm was obvious in the thermogram of FX5 proving TOL entrapment in the prepared flexosomes (Al-Mahallawi et al., 2015). Furthermore, the enthalpy of TOL melting peak was (81.32 mJ) which confirmed the drug crystallinity together with the sharpness of the peak. In contrast, the endothermic peak of TOL disappeared in the thermogram of FX5 with no enthalpy data at TOL at the melting point of TOL (122° C. There was a clear shift in the distinct endotherms of PC from 44.16 °C and 239.83 °C to 39.87 °C and 233.41 °C in FX5 thermogram. The individual peak of stearyl amine also appeared at lower temperature of 80.64 °C. The formation of less ordered lattice arrangement of flexosomes components might be responsible for these changes (Basha et al., 2013). Furthermore, the characteristic peak Cremophor RH 40 vanished in the thermogram of FX5 which confirmed its fluidization during flexosomes formation (Aziz et al., 2019) (Fig. 1S).

3.4. Ex vivo corneal permeation

The effect of flexosomes formulation on the permeability of TOL through excised rabbit cornea was investigated in comparison with TOL suspension. The cumulative amount of TOL permeated per unit area via FX5 and TOL suspension over time is graphically illustrated in Fig. 5. By calculating the permeability parameters (Table 5), it is clear that FX5 significantly increased TOL flux which resulted in increased total amount of the drug permeated over 8 h compared to TOL suspension ($P < 0.05$). This results in enhancement ratio of more than 3 for FX5 compared to drug suspension. This could be due to the nanometric size of flexosomes formulation which aided their permeation through the narrow network structure of the stroma in comparison with the coarse particles of TOL suspension (Zhou et al., 2017). In addition, Cremophor RH40, as edge activator, attracts preferentially to the aqueous humor and the vitreous due to its aqueous nature. Therefore, it facilitates deep penetration of flexosomes in the tissues of the eye (Kakkar & Kaur, 2011; Aziz et al., 2018). In addition to the previously mentioned advantages of its nanometric size and the presence of edge activator in its constructs in enhancing its corneal permeation, it was shown that the constructing phospholipid (PC) may have additional enhancement way into corneal tissues by direct phospholipid internalization and fusion with cell membrane (Rabinovich-Guilatt et al., 2004).

3.5. In vitro antifungal activity

3.5.1. Minimum inhibitory concentration

To test whether flexosomes formulation affects the antifungal activity of TOL, MIC, MFC and kill kinetics assays were performed. The minimum inhibitory concentration of FX5 was 0.24 μg/mL which was

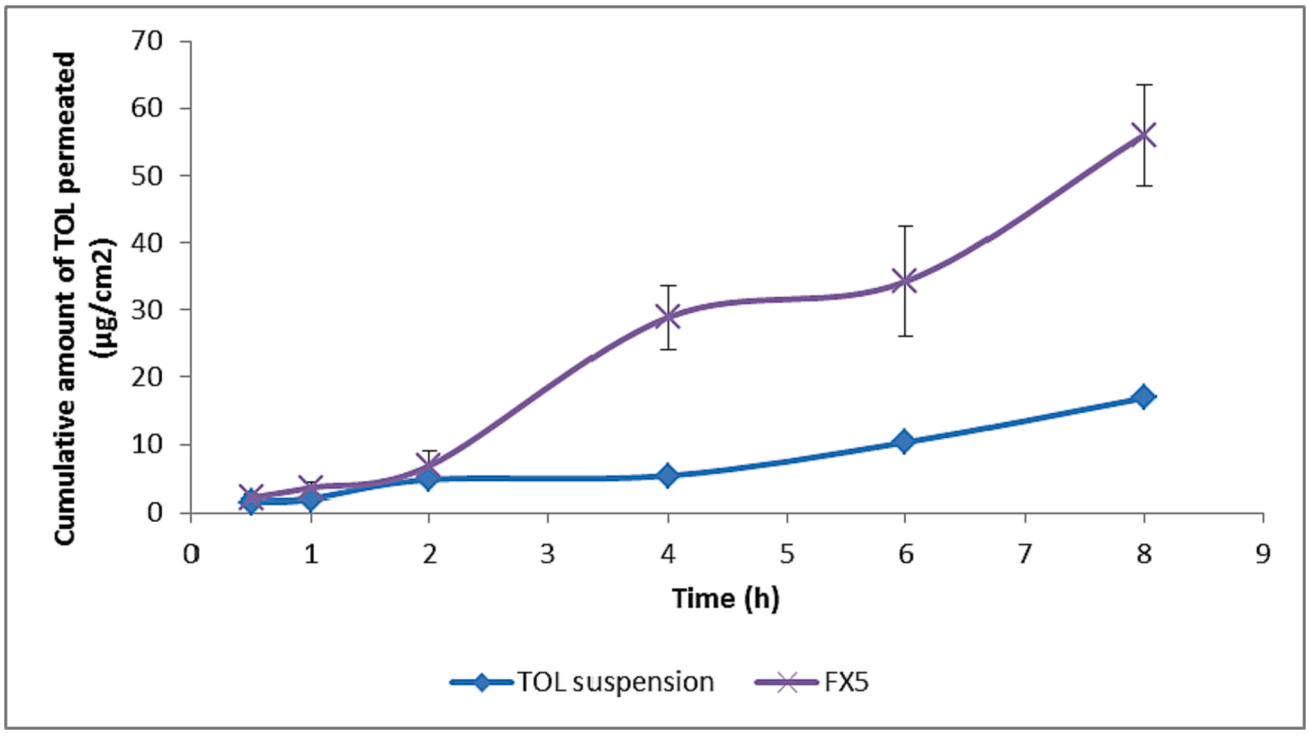

Fig. 5. Cumulative amount of TOL permeated per unit area across excised cornea via FX5 compared to drug suspension.

Table 5
Corneal permeability parameters of FX5 compared to drug suspension*.

Formula	Total amount of drug permeated in 24 h (µg/cm^2)*	J_{max} (µg/cm^2 × h)	ER
FX5	56.05 ± 7.55	10.95 ± 1.48	3.30
TOL suspension	16.92 ± 0.23	3.31 ± 0.05	1

* Abbreviations: J_{max}, Flux; ER, enhancement ratio.Data presented as mean ± SD (n = 3).

statistically lower than that of the TOL suspension (3.90 µg/mL) and placebo (250 µg/mL). This denotes the enhanced antifungal activity of FX5 compared to TOL suspension. This was most probably due to the enhanced drug solubility that promoted cell wall permeation and ergosterol synthesis inhibition which maximizes its antifungal efficiency (Li et al., 2018; Sayed et al., 2018).

3.5.2. Minimum fungicidal concentration

Both FX5 and TOL suspension showed fungicidal effect when incubated at 28 °C ± 2 for 48 h. The fungicidal effect of FX5 was more pronounced than TOL suspension (treatment B). FX5 showed MFC of 7.8 µg/mL (32.5x MIC) while MFC of TOL suspension (treatment B) was higher with a value of 125 µg/mL (32x MIC). These results support the superiority of TOL flexosomes antifungal effect compared to drug suspension.

3.5.3. Kill kinetics assay

Treatment A (FX5) eradicated *Aspergillus niger* (ATCC32656) after 10 h incubation at its MFC concentration (7.8 µg/mL) (32.5x MIC). On the other hand, treatment B (TOL suspension) couldn't kill *Aspergillus niger* (ATCC32656) but showed reduction in fungal colony count at its MFC concentration (125 µg/mL) (32x MIC) (Fig. 6).

3.6. In vivo studies

3.6.1. Draize test

FX5 didn't show any signs of inflammation at all tested time points compared to control eye. By the other words, FX5 scored zero on Draize scale which supported the safety and ocular tolerability of the optimal flexosomes.

3.6.2. Histopathology

Histopathology photomicrographs revealed the absence of abnormalities in the corneal tissues; the underlying stroma and endothelium and the lining corneal epithelium, as shown in Fig. 7 (a2). Same observation was shown in the retina, sclera and choroid (Fig. 7 (c2)) and iris (Fig. 7 (b2)), in comparison with untreated eyes (Fig. 7 (a1-c1)). Therefore, FX5 is safe and well-tolerated for ocular administration.

3.6.3. Susceptibility test

The antifungal activity of TOL is dependent on the retention time of the drug on the surface of the eye. Growth inhibition % imparted by FX5 increased gradually after 6 h of administration from 39.8 ± 6.79% to reach maximum inhibition at 24 h of administration (80.75 ± 9.55%), while TOL suspension showed no growth inhibition till 24 h of administration to reach 58.85 ± 9.7% (Fig. 8). Growth inhibition of FX5 was greater than TOL suspension after 6 h and 8 h of administration (P = 0.026 and 0.023, respectively) (one way ANOVA, $P < 0.05$). FX5 imparted sustained antifungal activity of TOL a longer time in comparison with TOL suspension with an area under the curve 1.28 folds higher than that of TOL suspension ($AUC_{2h\text{-}24h}$ = 1306 and 1022, respectively). This is most probably due to the presence of stearyl amine (positive charge inducer) in FX5 construct which has an important role to increase the viscosity of the formulation and consequently prolong the retention time when applied to the eye surface. In another word, flexosomes (being positively charged vesicles) can intimately adhere to the negatively charged cornea and consequently cause prolonged

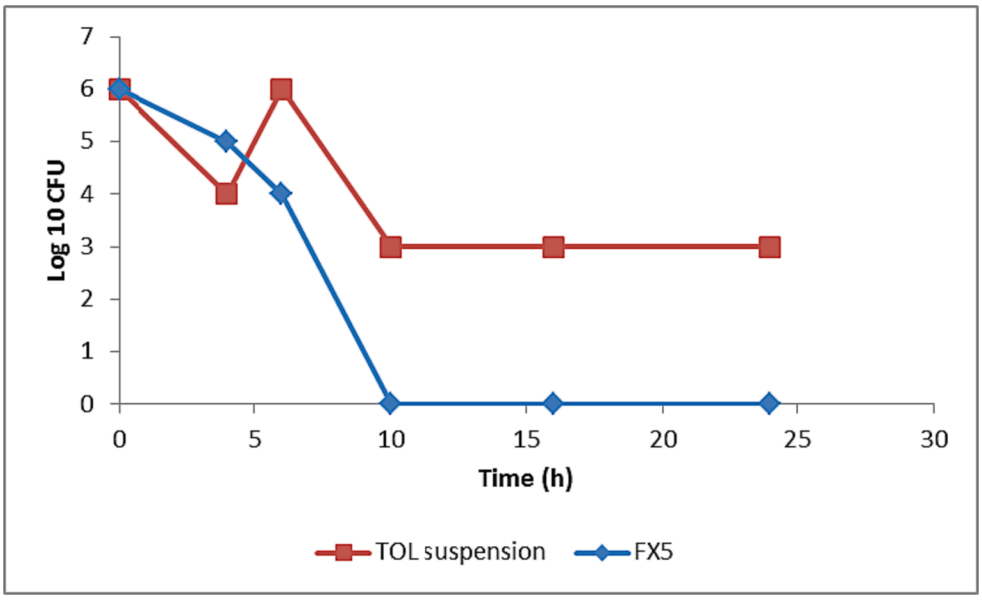

Fig. 6. The killing kinetics of treatment A (FX5) and treatment B (TOL suspension) tested against Aspergillus niger (ATCC32656). Treatment A tested at concentration of (7.8 μg/mL) (32.5x MIC), treatment B (TOL suspension) tested at concentration of (125 μg/mL) (32x MIC). Data is represented by means of the number of recovered colonies counted at each time point ± SD, n = 3. The chart was generated using GraphPad Prism (v5).

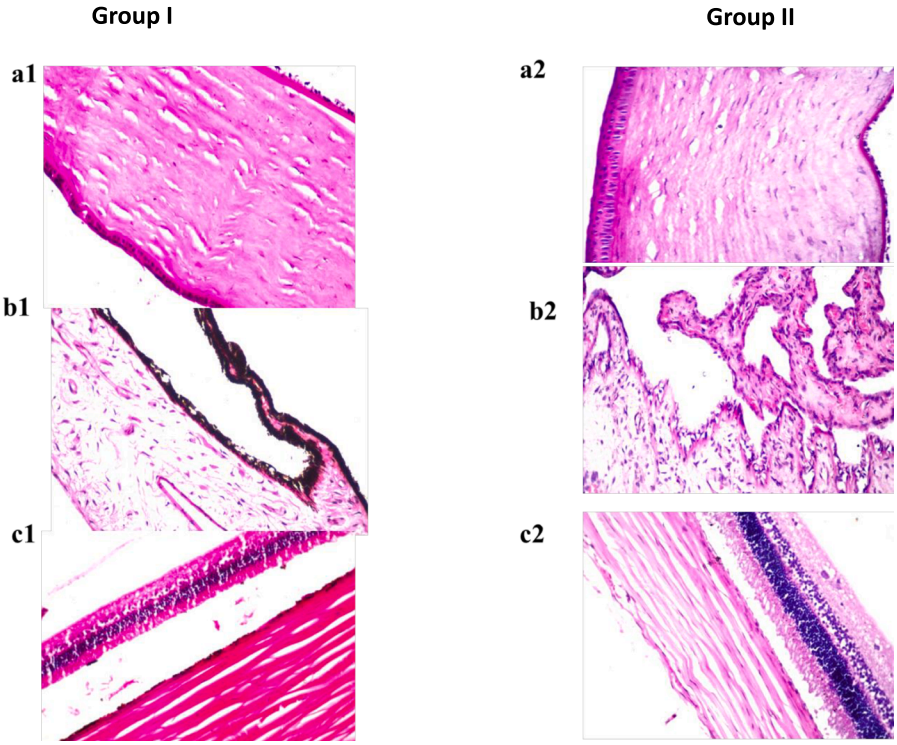

Fig. 7. Photomicrographs showing histopathological sections (hematoxylin and eosin stained) of normal untreated rabbit eye (group I) and rabbit eye treated with FX5 (group II); where a1 and a2 represent the cornea showing normal histopathological structure of corneal epithelium, stroma and endothelium at magnification power of x40, while b1 and b2 represent the iris and c1 and c2 represent the retina, choroid and sclera with normal histopathological structure at the same magnification power.

residence time. In contrast, drug suspension showed poor antifungal properties as it is easily washed off and diluted with tear turnover. Hence, the enhanced antifungal activity was mainly due to the increased corneal loading rather than the prolonged release of TOL (Rabinovich-Guilatt et al., 2004).

4. Conclusion

In the present work, flexosomes were fashioned as a novel nano-system for enhanced ocular delivery of TOL. A full $3^1.2^2$ factorial design was selected to investigate the effect of formulation factors on flexosomes properties. FX5, prepared using 20 mg stearylamine, 5 mL

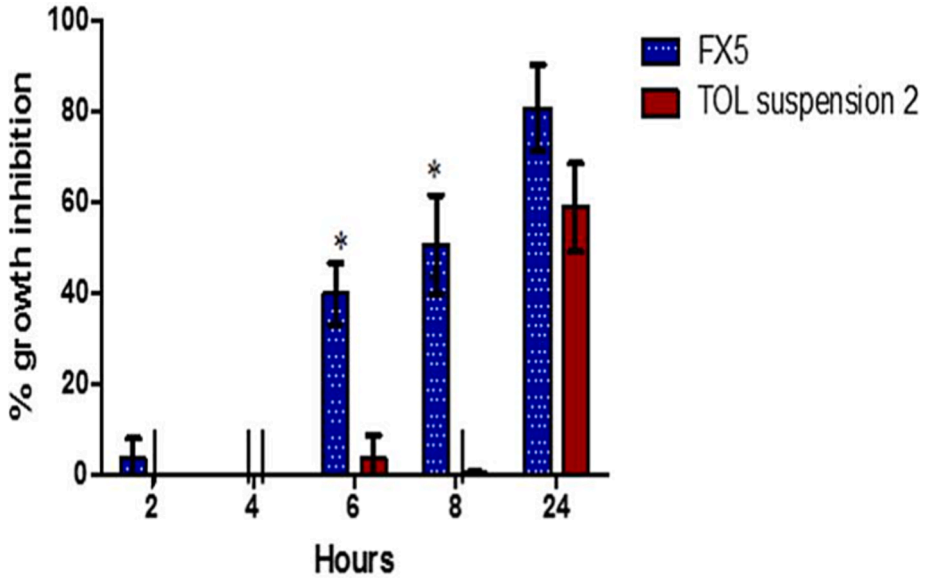

Fig. 8. Percentage growth inhibition of *Aspergillus niger* (ATCC32656) by FX5 (treatment A) compared to TOL suspension (treatment B) in rabbit external ocular tissue. Data represent the means of % growth inhibition after time interval (2 – 24 h) of administration ± SD, n = 3 (one-way ANOVA, p-value < 0.05). (*) Means statistically significant difference exists between columns. (II) indicates no bar (0 % growth inhibition). The chart was generated using GraphPad Prism (v5).

hydration medium and Cremophor RH 40 as edge activator, was selected as the optimal TOL flexosomes with desirability value of 0.817. FX5 showed high encapsulation efficiency, small particle size and spherical morphology. Ex vivo permeation study was conducted in which FX5 was compared to TOL suspension and showed superior drug flux and more enhanced corneal permeation potential. Furthermore, histopathological testing showed the tolerability and safety and of FX5 for ocular application. The in vivo susceptibility test assured the superior residence of flexosomes on the eye surface compared to drug suspension. Therefore, the study suggests that FX5 might be a breakthrough for enhanced TOL ocular delivery for fungal keratitis treatment with superior antifungal effect.

CRediT authorship contribution statement

Diana Aziz: Conceptualization, Investigation, Visualization, Resources. **Sally Mohamed:** Conceptualization, Investigation, Resources, Writing – original draft. **Saadia Tayel:** Supervision. **Amal Makhlouf:** Conceptualization, Investigation, Visualization, Resources, Supervision.

Declaration of Competing Interest

The authors declare that they have no known competing financial interests or personal relationships that could have appeared to influence the work reported in this paper.

Data availability

No data was used for the research described in the article.

Appendix A. Supplementary data

Supplementary data to this article can be found online at https://doi.org/10.1016/j.ijpharm.2023.123471.

References

Abdelbary, G., 2011. Ocular ciprofloxacin hydrochloride mucoadhesive chitosan-coated liposomes. Pharm. Dev. Technol. 16, 44–56.
Abdelbary, A.A., Aboughaly, M.H., 2015. Design and optimization of topical methotrexate loaded niosomes for enhanced management of psoriasis: application of Box-Behnken design, in-vitro evaluation and in-vivo skin deposition study. Int. J. Pharm. 485, 235–243.
Abdelbary, G.A., Aburahma, M.H., 2015. Oro-dental mucoadhesive proniosomal gel formulation loaded with lornoxicam for management of dental pain. J. Liposome Res. 25, 107–121.
Abd-Elsalam, W.H., El-Zahaby, S.A., Al-Mahallawi, A.M., 2018. Formulation and in vivo assessment of terconazole-loaded polymeric mixed micelles enriched with Cremophor EL as dual functioning mediator for augmenting physical stability and skin delivery. Drug Deliv. 25, 484–492.
Abousamra, M.M., Mohsen, A.M., 2016. Solid lipid nanoparticles and nanostructured lipid carriers of tolnaftate: design, optimization and in-vitro evaluation. Int J Pharm Pharm Sci 8, 380–385.
Agarwal, R., Iezhitsa, I., Agarwal, P., Abdul Nasir, N.A., Razali, N., Alyautdin, R., Ismail, N.M., 2016. Liposomes in topical ophthalmic drug delivery: an update. Drug Deliv. 23, 1075–1091.
Akhtar, N., Sahu, S., Pathak, K., 2016. Antifungal potential of tolnaftate against Candida albicans in the treatment of onychomycosis: development of nail lacquer and ex vivo characterization. Pharm Biomed Res 2, 1–12.
Alastruey-Izquierdo, A., Melhem, M.S., Bonfietti, L.X., Rodriguez-Tudela, J.L., 2015. Susceptibility test for fungi: clinical and laboratorial correlations in medical mycology. Rev. Inst. Med. Trop. Sao Paulo 57, 57–64.
Albash, R., Al-Mahallawi, A.M., Hassan, M., Alaa-Eldin, A.A., 2021. Development and optimization of terpene-enriched vesicles (Terpesomes) for effective ocular delivery of fenticonazole nitrate: in vitro characterization and in vivo assessment. Int. J. Nanomed. 16, 609.
Al-Mahallawi, A.M., Khowessah, O.M., Shoukri, R.A., 2014. Nano-transfersomal ciprofloxacin loaded vesicles for non-invasive trans-tympanic ototopical delivery: in-vitro optimization, ex-vivo permeation studies, and in-vivo assessment. Int. J. Pharm. 472, 304–314.
Al-Mahallawi, A.M., Abdelbary, A.A., Aburahma, M.H., 2015. Investigating the potential of employing bilosomes as a novel vesicular carrier for transdermal delivery of tenoxicam. Int. J. Pharm. 485, 329–340.
Arunothayanun, P., Bernard, M.S., Craig, D.Q., Uchegbu, I.F., Florence, A.T., 2000. The effect of processing variables on the physical characteristics of non-ionic surfactant vesicles (niosomes) formed from a hexadecyl diglycerol ether. Int. J. Pharm. 201, 7–14.
Aziz, D.E., Abdelbary, A.A., Elassasy, A.I., 2018. Fabrication of novel elastosomes for boosting the transdermal delivery of diacerein: statistical optimization, ex-vivo permeation, in-vivo skin deposition and pharmacokinetic assessment compared to oral formulation. Drug Deliv. 25, 815–826.
Aziz, D.E., Abdelbary, A.A., Elassasy, A.I., 2019. Investigating superiority of novel bilosomes over niosomes in the transdermal delivery of diacerein: in vitro characterization, ex vivo permeation and in vivo skin deposition study. J. Liposome Res. 29, 73–85.
Aziz, D., Mohamed, S., Tayel, S., Makhlouf, A., 2022a. Implementing polymeric pseudorotaxanes for boosting corneal permeability and antiaspergillus activity of tolnaftate: formulation development, statistical optimization, ex vivo permeation and in vivo assessment. Drug Deliv. 29, 2162–2176.
Aziz, D., Mohamed, S.A., Tayel, S., Makhlouf, A., 2022b. Enhanced Ocular Anti-Aspergillus Activity of Tolnaftate Employing Novel Cosolvent-Modified Spanlastics: Formulation, Statistical Optimization, Kill Kinetics, Ex Vivo Trans-Corneal

Permeation, In Vivo Histopathological and Susceptibility Study. Pharmaceutics 14, 1746.
Balakrishnan, P., Shanmugam, S., Lee, W.S., Lee, W.M., Kim, J.O., Oh, D.H., Kim, D.D., Kim, J.S., Yoo, B.K., Choi, H.G., Woo, J.S., Yong, C.S., 2009. Formulation and in vitro assessment of minoxidil niosomes for enhanced skin delivery. Int. J. Pharm. 377, 1–8.
Bancroft, J., Stevens, A., Turner, D., 1996. Theory and practice of histopathological techniques 4th eds. Churchill Livingstone, New York, London and Madrid.
Basha, M., Abd El-Alim, S.H., Shamma, R.N., Awad, G.E., 2013. Design and optimization of surfactant-based nanovesicles for ocular delivery of Clotrimazole. J. Liposome Res. 23, 203–210.
Di Marzio, L., Marianecci, C., Rinaldi, F., Esposito, S., Carafa, M., 2012. Deformable surfactant vesicles loading ammonium glycyrrhizinate: characterization and in vitro permeation studies. Lett. Drug Des. Discovery 9, 494–499.
El Zaafarany, G.M., Awad, G.A., Holayel, S.M., Mortada, N.D., 2010. Role of edge activators and surface charge in developing ultradeformable vesicles with enhanced skin delivery. Int. J. Pharm. 397, 164–172.
Eldeeb, A.E., Salah, S., Ghorab, M., 2019. Formulation and evaluation of cubosomes drug delivery system for treatment of glaucoma: ex-vivo permeation and in-vivo pharmacodynamic study. J Drug Deliv Sci Technol 52, 236–247.
Elmeshad, A.N., Mohsen, A.M., 2016. Enhanced corneal permeation and antimycotic activity of itraconazole against Candida albicans via a novel nanosystem vesicle. Drug Deliv. 23, 2115–2123.
El-Ridy, M.S., Abdelbary, A., Essam, T., Abd El-Salam, R.M., Aly Kassem, A.A., 2011. Niosomes as a potential drug delivery system for increasing the efficacy and safety of nystatin. Drug Dev. Ind. Pharm. 37, 1491–1508.
Fahmy, A.M., El-Setouhy, D.A., Ibrahim, A.B., Habib, B.A., Tayel, S.A., Bayoumi, N.A., 2018. Penetration enhancer-containing spanlastics (PECSs) for transdermal delivery of haloperidol: in vitro characterization, ex vivo permeation and in vivo biodistribution studies. Drug Deliv. 25, 12–22.
Fares, A.R., Elmeshad, A.N., MaA, K., 2018. Enhancement of dissolution and oral bioavailability of lacidipine via pluronic P123/F127 mixed polymeric micelles: formulation, optimization using central composite design and in vivo bioavailability study. Drug Deliv. 25, 132–142.
Fetih, G., 2016. Fluconazole-loaded niosomal gels as a topical ocular drug delivery system for corneal fungal infections. J Drug Deliv Sci Technol 35, 8–15.
Gonzalez-Rodriguez, M.L., Arroyo, C.M., Cozar-Bernal, M.J., Gonzalez, R.P., Leon, J.M., Calle, M., Canca, D., Rabasco, A.M., 2016. Deformability properties of timolol-loaded transfersomes based on the extrusion mechanism. Statistical optimization of the process. Drug Dev. Ind. Pharm. 42, 1683–1694.
Gupta, A., Aggarwal, G., Singla, S., Arora, R., 2012. Transfersomes: a novel vesicular carrier for enhanced transdermal delivery of sertraline: development, characterization, and performance evaluation. Sci. Pharm. 80, 1061–1080.
Hichmah, H.N., 2019. Effect of Surfactant Concentration on the Entrapment Efficiency Niosomes Aqueous Extract of Cassava Leaves (Manihot esculenta Crantz). Asian Journal of Pharmaceutics (AJP): Free full text articles from Asian J Pharm 13.
Honary, S., Zahir, F., 2013. Effect of zeta potential on the properties of nano-drug delivery systems-a review (Part 2). Trop. J. Pharm. Res. 12, 265–273.
Humphries, R.M., Ambler, J., Mitchell, S.L., Castanheira, M., Dingle, T., Hindler, J.A., Koeth, L., Sei, K., 2018. CLSI methods development and standardization working group best practices for evaluation of antimicrobial susceptibility tests. J. Clin. Microbiol. 56, e01934–e02017.
Ismail, M.M., Samir, R., Saber, F.R., Ahmed, S.R., Farag, M.A., 2020. Pimenta oil as a potential treatment for Acinetobacter baumannii wound infection: In vitro and in vivo bioassays in relation to its chemical composition. Antibiotics 9, 679.
Junyaprasert, V.B., Teeranachaideekul, V., Supaperm, T., 2008. Effect of charged and non-ionic membrane additives on physicochemical properties and stability of niosomes. AAPS PharmSciTech 9, 851–859.
Kakkar, S., Kaur, I.P., 2011. Spanlastics–a novel nanovesicular carrier system for ocular delivery. Int. J. Pharm. 413, 202–210.
Kaur, I.P., Rana, C., Singh, H., 2008. Development of effective ocular preparations of antifungal agents. J. Ocul. Pharmacol. Ther. 24, 481–493.
Kezutyte, T., Kornysova, O., Maruska, A., Briedis, V., 2010. Assay of tolnaftate in human skin samples after in vitro penetration studies using high performance liquid chromatography. Acta Pol. Pharm. 67, 327–334.
Khalil, R.M., Abdelbary, G.A., Basha, M., Awad, G.E., El-Hashemy, H.A., 2017. Design and evaluation of proniosomes as a carrier for ocular delivery of lomefloxacin HCl. J. Liposome Res. 27, 118–129.
Kumari, P., Misra, S., Pandey, S., 2017. Formulation and Evaluation of Tolnaftate Microsponges Loaded Gels for Treatment of Dermatophytosis. European Journal of Pharmaceutical and Medical Research 4, 326–335.
Law, S.L., Huang, K.J., Chiang, C.H., 2000. Acyclovir-containing liposomes for potential ocular delivery. Corneal penetration and absorption. J. Control. Release 63, 135–140.
Li, J., Li, Z., Liang, Z., Han, L., Feng, H., He, S., Zhang, J., 2018. Fabrication of a drug delivery system that enhances antifungal drug corneal penetration. Drug Deliv. 25, 938–949.
Naguib, S.S., Hathout, R.M., Mansour, S., 2017. Optimizing novel penetration enhancing hybridized vesicles for augmenting the in-vivo effect of an anti-glaucoma drug. Drug Deliv. 24, 99–108.
Naguib, M.J., Makhlouf, A.I., 2021. Scalable flibanserin nanocrystal-based novel sublingual platform for female hypoactive sexual desire disorder: engineering, optimization adopting the desirability function approach and in vivo pharmacokinetic study. Drug Deliv. 28, 1301–1311.
Nour, S.A., Abdelmalak, N.S., Naguib, M.J., Rashed, H.M., Ibrahim, A.B., 2016. Intranasal brain-targeted clonazepam polymeric micelles for immediate control of status epilepticus: in vitro optimization, ex vivo determination of cytotoxicity, in vivo biodistribution and pharmacodynamics studies. Drug Deliv. 23, 3681–3695.
Rabinovich-Guilatt, L., Couvreur, P., Lambert, G., Dubernet, C., 2004. Cationic vectors in ocular drug delivery. J. Drug Target. 12, 623–633.
Ruckmani, K., Sankar, V., 2010. Formulation and optimization of Zidovudine niosomes. AAPS PharmSciTech 11, 1119–1127.
Sayed, S., Elsayed, I., Ismail, M.M., 2018. Optimization of β-cyclodextrin consolidated micellar dispersion for promoting the transcorneal permeation of a practically insoluble drug. Int. J. Pharm. 549, 249–260.
Sherwal, B., Verma, A., 2008. Epidemiology of ocular infection due to bacteria and fungus-a prospective study. JK Sci. 10, 127–131.
Spadea, L., Giannico, M.I., 2019. Diagnostic and management strategies of Aspergillus endophthalmitis: current insights. Clin. Ophthalmol. 13, 2573.
Varshosaz, J., Mohammadi Ghalaei, P., Hassanzadeh, F. 2014. Hyaluronate targeted solid lipid nanoparticles of etoposide: optimization and in vitro characterization. Journal of Nanomaterials 2014.
Varshosaz, J., Pardakhty, A., Hajhashemi, V.I., Najafabadi, A.R., 2003. Development and physical characterization of sorbitan monoester niosomes for insulin oral delivery. Drug Deliv. 10, 251–262.
Yeo, L.K., Chaw, C.S., Elkordy, A.A., 2019. The Effects of Hydration Parameters and Co-Surfactants on Methylene Blue-Loaded Niosomes Prepared by the Thin Film Hydration Method. Pharmaceuticals (Basel) 12.
Younes, N.F., El Assasy, A.-E.-H.-I., Makhlouf, A.I., 2021. Microenvironmental pH-modified Amisulpride-Labrasol matrix tablets: development, optimization and in vivo pharmacokinetic study. Drug Deliv. Transl. Res. 11, 103–117.
Yousry, C., Zikry, P.M., Salem, H.M., Basalious, E.B., El-Gazayerly, O.N., 2020. Integrated nanovesicular/self-nanoemulsifying system (INV/SNES) for enhanced dual ocular drug delivery: statistical optimization, in vitro and in vivo evaluation. Drug Deliv. Transl. Res. 10, 801–814.
Yusuf, M., Sharma, V., Pathak, K., 2014. Nanovesicles for transdermal delivery of felodipine: Development, characterization, and pharmacokinetics. Int J Pharm Investig 4, 119–130.
Zhou, T., Zhu, L., Xia, H., He, J., Liu, S., He, S., Wang, L., Zhang, J., 2017. Micelle carriers based on macrogol 15 hydroxystearate for ocular delivery of terbinafine hydrochloride: In vitro characterization and in vivo permeation. Eur. J. Pharm. Sci. 109, 288–296.
Zhu, P., Li, Y., Guo, T., Liu, S., Tancer, R.J., Hu, C., Zhao, C., Xue, C., Liao, G., 2023. New antifungal strategies: drug combination and co-delivery. Advanced Drug Delivery. Reviews:114874.